

## Effect of Magnetic Ion Doping on Structural, Electric and Relaxor Properties of $\text{Pb}(\text{Fe}_{2/3}\text{W}_{1/3})\text{O}_3$ Multiferroic Ceramics

*Bárbara Fraygola<sup>a\*</sup>, José Antônio Eiras<sup>b</sup>*

<sup>a</sup>Ceramics Laboratory, EPFL - Swiss Federal Institute of Technology, 1015- Lausanne, Switzerland

<sup>b</sup>Grupo de Cerâmicas Ferroelétricas, Departamento de Física, Universidade Federal de São Carlos – UFSCar, Rodovia Washington Luiz, Km 235, Caixa Postal 676, CEP 13565-905, São Carlos, SP, Brasil

Received: July 4, 2014; Revised: September 29, 2014

Single-phase  $\text{Pb}(\text{Fe}_{2/3}\text{W}_{1/3})\text{O}_3$  (PFW) multiferroic ceramics doped with magnetic ions were fabricated using a modified B-site precursor method. Dielectric response was investigated over a wide range of temperature and frequency. Doping did not modify the characteristic temperatures ( $T_C$ ,  $T_N$ ) and the order at ferroelectric phase transition, keeping the relaxor properties. However, the leakage current and resistivity of PFW have been improved with the substitutions: 1 mol%  $\text{MnO}_2$  addition caused a significant increase in the electric resistivity of PFW ceramics, around 7 orders of magnitude.

**Keywords:** multiferroic, PFW, ferroelectric, microwave frequencies, relaxor

### 1. Introduction

As is well known, PZT ( $\text{Pb}(\text{Zr}_x\text{Ti}_{1-x})\text{O}_3$ ) as a ferroelectric system can be improved by changing the composition in order to make it suitable for technological applications, such as piezoelectric transducers, pyroelectric detectors, and nonvolatile ferroelectric memories<sup>1-3</sup>. In the same way, multiferroic materials, in which electric and magnetic orderings coexist in a single phase, have attracted the attention of the scientific community<sup>4,5</sup>. These materials have great potential for creation of magnetoelectric and magneto-optical devices and the simultaneous occurrence of electric and magnetic orderings in the same phase have made multiferroic materials interesting for technology in information storage and sensors. However, there is a scarcity of materials exhibiting multiferroic behavior,<sup>6,7</sup> and, generally, they have some inherent problems, characterized predominantly by a high leakage current, due to the existence of a large numbers of charge carriers, mainly attributed to oxygen vacancies or Pb evaporation during the sintering process, which makes difficult to achieve high electric resistivity<sup>4,5,8</sup>. In order to overcome these problems, doping appears as a possible option.

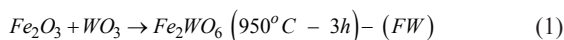
In particular, lead iron tungstate ( $\text{Pb}(\text{Fe}_{2/3}\text{W}_{1/3})\text{O}_3$  - PFW) has been studied looking for applications in dielectrics for capacitors, due to the high relative dielectric permittivity, relaxor properties, low sintering temperatures (below 900°C). Otherwise PFW presents conditions for the coexistence of ferroelectricity and magnetism, due to the presence of two kinds of cations ( $\text{Fe}^{3+}$  and  $\text{W}^{6+}$ ) randomly distribute at the octahedral B-site positions. PFW is ferroelectric ( $T_C \sim 180\text{K}$ ) and antiferromagnetic ( $T_N \sim 340\text{K}$ )<sup>9</sup>. An interesting peculiarity of the PFW system, by comparison with other multiferroic materials, is caused by the presence of magnetic ions  $\text{Fe}^{3+}$  with occupancy of 66.66% of the B-octahedral sites of the perovskite cells,

leading to one of highest magnetic ordering temperature<sup>10</sup>. However, in multiferroic materials, a superposition between ferroelectric ordering and electric conductivity can occur when polyvalent cations, e.g., Fe, Mn or Cu, are incorporated. For example, the electron transferred between mixed valence states,  $\text{Fe}^{3+}$  and  $\text{Fe}^{2+}$ , may lead to an increase in the electric conductivity. High electrical conductivity can mask Curie points, phase transition temperatures and ferroelectric domain reorientation measurements.

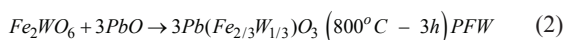
In this context, the present work aims to study the influence of magnetic ions addition on the phase transition and relaxor characteristics of PFW ceramics. The dielectric response for non-doped and Mn, Cr and Gd -doped PFW is analyzed in the frequency and temperature domain. The changes in the diffuse phase transition, electric conductivity and relaxor character by the addition of magnetic ions are discussed. Dielectric properties at high frequencies (microwave region) permitted us to characterize the dielectric response and magnetic phase transitions without conductive influences.

### 2. Experimental Procedure

A two-stage solid-state reaction, synthesis process similar to that used by Swartz and Shrouf<sup>11</sup> to fabricate perovskite lead manganese niobate (PMN), was used in this work to prepare the PFW ceramics. In this case,  $\text{Fe}_2\text{O}_3$  was first reacted with  $\text{WO}_3$  to produce  $\text{Fe}_2\text{WO}_6$ , followed by a second reaction between the  $\text{Fe}_2\text{WO}_6$  and  $\text{PbO}$ , according the solid-reactions sequence:



in the first stage and:



at the second stage.

\*e-mail: barbarafraygola@gmail.com

Fe<sub>2</sub>O<sub>3</sub> (99.99%, Alfa) and WO<sub>3</sub> (99.8%, Alfa) were mixed in distilled H<sub>2</sub>O media for 2 h, and then dried and preheated at 850°C, 950°C and 1000°C for 3 h to study the phase formation of Fe<sub>2</sub>WO<sub>6</sub>. Afterward ground milling for 5 hs, PbO (99.99%, GFS Chemicals) was mixed in a stoichiometric ratio to Fe<sub>2</sub>WO<sub>6</sub> in distilled H<sub>2</sub>O media for 1 h. The mixture was initially calcined at 800°C for 3 h and reground for 5h in distilled H<sub>2</sub>O media. After, part of the reaction product PFW was mixed with Cr<sub>2</sub>O<sub>3</sub>, Gd<sub>2</sub>O<sub>3</sub> or MnO<sub>2</sub> (1% weight) and re- calcined at 800°C for 3h. Such a synthesis procedure enhances the efficiency of the formation of the desired perovskite phase. Ceramic bodies were prepared by adding 3wt% polyvinyl alcohol (PVA) binder to the calcined powders, prior to pressing as pellets, with 10 mm in diameter and 1-2 mm thickness, in a 100 MPa pseudo-uniaxial die and then isostatically. Finally the pellets have been sintered at 830°C for 5 h in an alumina crucible. The pellets were covered with powder of the same composition, in order to reduce the Pb-evaporation during the sintering process. The temperature ramps were controlled at 5°C/min for heating up and 2°C/min for cooling down. Analysis performed by EDX and SEM confirmed the compositional stoichiometry and microstructural homogeneity for all compositions. The crystallinity, present phases and symmetry of all samples was checked by XRD using a least mean square method to find the cell parameters. The X-ray powder diffraction patterns were obtained at room temperature on a Rigaku Denki powder diffractometer with geometry  $\theta$ -2 $\theta$ , rotating anode X-ray source (Cu K $\alpha$  radiation,  $\lambda = 1.542 \text{ \AA}$ ), and scintillation detector.

The relative densities of the sintered samples were determined by the Archimedes method, while their morphological features were analyzed in a Jeol/5800LV scanning electron microscope (SEM). The sintered ceramic bodies were cut in disc form and polished to a thickness of 0.5 mm and 2mm of diameter for dielectric measurements. After that, they were annealed at 873 K for 0.5 h to release mechanical stresses introduced during the polishing. Gold electrodes were sputtered on the samples. Dc resistivity was measured by a two probe method, applying low voltages, using a 6517A Keithley electrometer. Microwave dielectric measurements were carried out in the temperature range of 80-420 K (network analyzer HP-8719C), while RF measurements (HP 4194A) were performed in the range 15-600 K.

### 3. Results

Table 1 presents physical characteristics of the investigated samples. It can be seen that densities of about 96-99% of the theoretic values (8.91g/cm<sup>3</sup> for pure PFW)

were achieved. The theoretic densities were calculated considering the nominal composition and the cell volume obtained from the XRD patterns, assuming a cubic symmetry. The highest density was obtained for the sample containing MnO<sub>2</sub>, indicating that the addition of Mn ions helps to increase the densification of the samples. Lattice parameter listed in Table 1 show that doping decreases the unit cell volume. As can be seen in Figure 1, room temperature XRD patterns of the PFW ceramics indicate the formation of a majority PFW perovskite phase, to a first approximation, with a cubic perovskite-type structure with space group symmetry  $pm\bar{3}m$ . A minor phase (In Figure 1 (\*) CrPb<sub>2</sub>O<sub>5</sub> and MnPb<sub>2</sub>O<sub>4</sub>) could be detected, only for the sample doped with Cr<sub>2</sub>O<sub>3</sub> and MnO<sub>2</sub>, indicating that 1% is already above the limit of solubility of these oxides in PFW.

High degrees of densification is also inferred by the SEM observation (Figure 2). The microstructure in Figure 2 shows an average grain size around 2-3  $\mu\text{m}$  for all samples and no systematic variation of grain size with doping

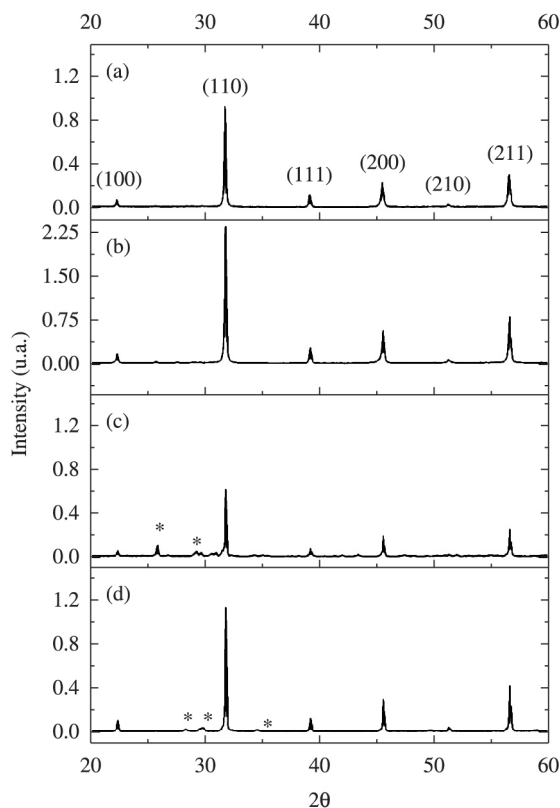


**Figure 1.** XRD patterns for sintered (a) PFW, (b) PFW-1% Cr<sub>2</sub>O<sub>3</sub>, (c) PFW-1% Gd<sub>2</sub>O<sub>3</sub> and (d) PFW-1%MnO<sub>2</sub> ceramics.

**Table 1.** Relative density, Lattice parameter and electric (DC) resistivity for sintered PFW, PFW-1% Gd<sub>2</sub>O<sub>3</sub>, PFW-1% Cr<sub>2</sub>O<sub>3</sub> and PFW-1%MnO<sub>2</sub> ceramics.

Sample	% Relative density	Lattice parameter (Å)	Electric Resistivity (Ω.m)
PFW	98%	3.98837	1.1X10 <sup>4</sup>
PFW-MnO <sub>2</sub>	99%	3.98171	2.0X10 <sup>11</sup>
PFW-Cr <sub>2</sub> O <sub>3</sub>	96%	3.97808	5.0X10 <sup>6</sup>
PFW-Gd <sub>2</sub> O <sub>3</sub>	97%	3.97765	8.3X10 <sup>4</sup>

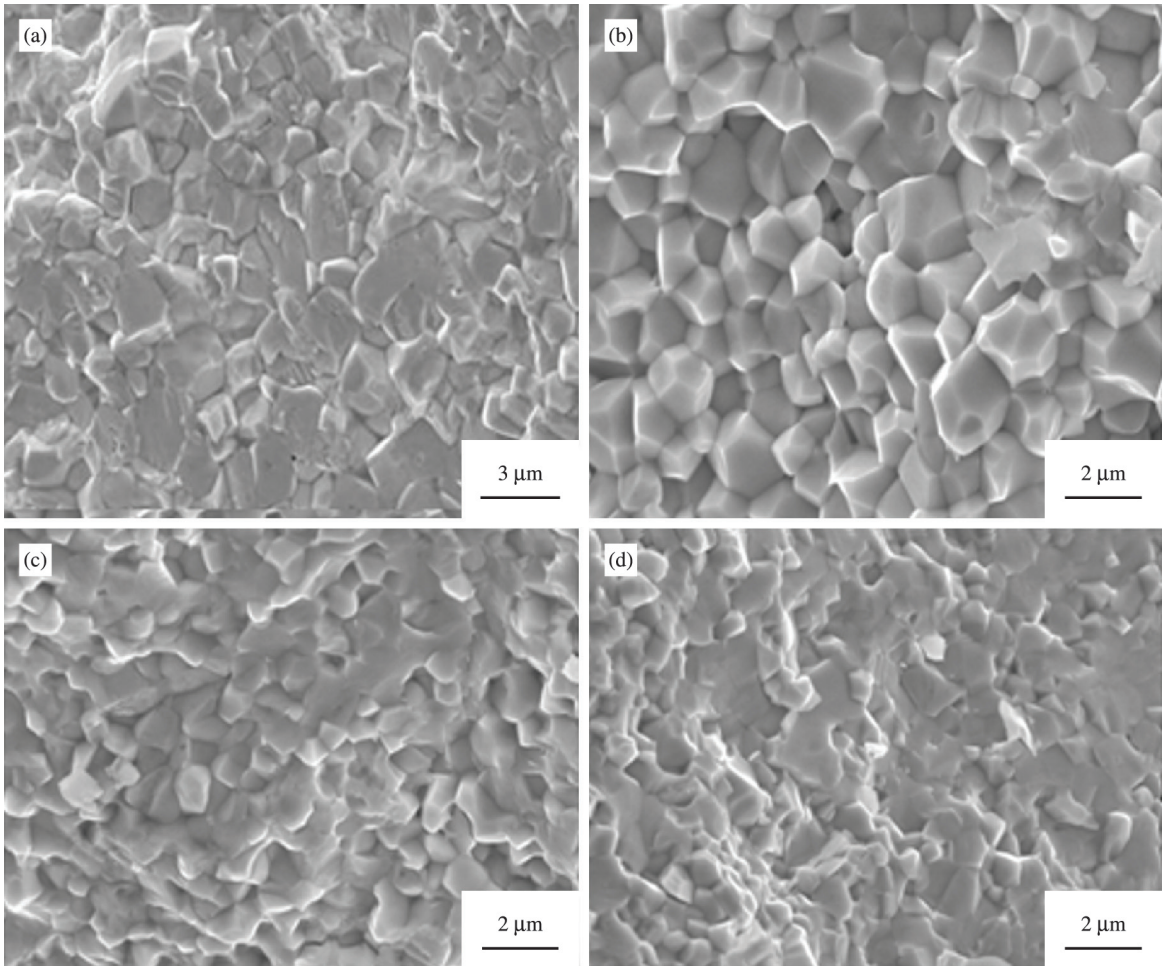


**Figure 2.** SEM micrograph of (a) PFW, (b) PFW-1%  $Gd_2O_3$ , (c) PFW-1%  $Cr_2O_3$  and (d) PFW-1%  $MnO_2$  ceramics. The magnification factor of the SEM is 6000x.

element was observed. However, the “pure” or  $MnO_2$  and  $Gd_2O_3$  doped samples have a mix characteristic between intergranular and transgranular fracture, where the last is the predominant. In the case of  $Cr_2O_3$  intergranular fracture is characteristic. Again, this phenomenon can be related to the extra chromium phase ( $CrPb_2O_3$ ). However, it was not observed for the  $MnO_2$  doped sample.

The room temperature dc electric resistivity for the PFW based ceramics are also listed in Table 1. All compositions showed relatively high conductivity, except the manganese doped sample. In this case occurs an increase in resistivity from  $10^4$  to  $10^{11}$   $\Omega.m$ , when comparing with the pure sample.

In Figures 3a-d the relative dielectric permittivity ( $\epsilon_r$  – real  $\epsilon'$  and imaginary  $\epsilon''$  components) for PFW, PFW doped with 1 mol% of  $MnO_2$ ,  $Gd_2O_3$  or  $Cr_2O_3$ , respectively, are shown as a function of temperature at RF frequencies ranging from 1 KHz to 1 MHz.

In the temperature range 150–400 K real and imaginary components present a strong frequency dependence. For the imaginary component, the peak around 180 K, which can be attributed to the ferroelectric–paraelectric transition (FE), increases the temperature of the maximum with the

measuring frequency (Figure 3a). This indicates a diffuse character of the phase transition, typical for relaxors.

The dispersion observed in the real and imaginary part in Figure 3, at temperatures higher than those related to the FE transition (in the range 200–400 K), shift as well towards higher temperatures with increasing frequency. The maximum permittivity values decrease with raising frequencies suggesting that are originated from thermally activated relaxation process. These phenomena, superposed to the dielectric contribution, are assumed to be related with hopping conductivity mechanisms.

In this work  $T_c$  was practically not altered with  $Cr_2O_3$  and  $Gd_2O_3$  doping ( $\sim 190$  K at 1 MHz), but 1%  $MnO_2$  reduces the transition temperature from 184 K to 165 K. Likewise, the addition of manganese decreases and moves to high temperatures the conductive contribution above the ferroelectric transition. This phenomenon agrees with the increase of electrical dc resistivity for this kind of doping. The influence of the added dopants on the temperature and absolute values of the maximum dielectric permittivity, corresponding to the ferroelectric–paraelectric transition is consistent with the results reported by Miranda,<sup>12</sup> who

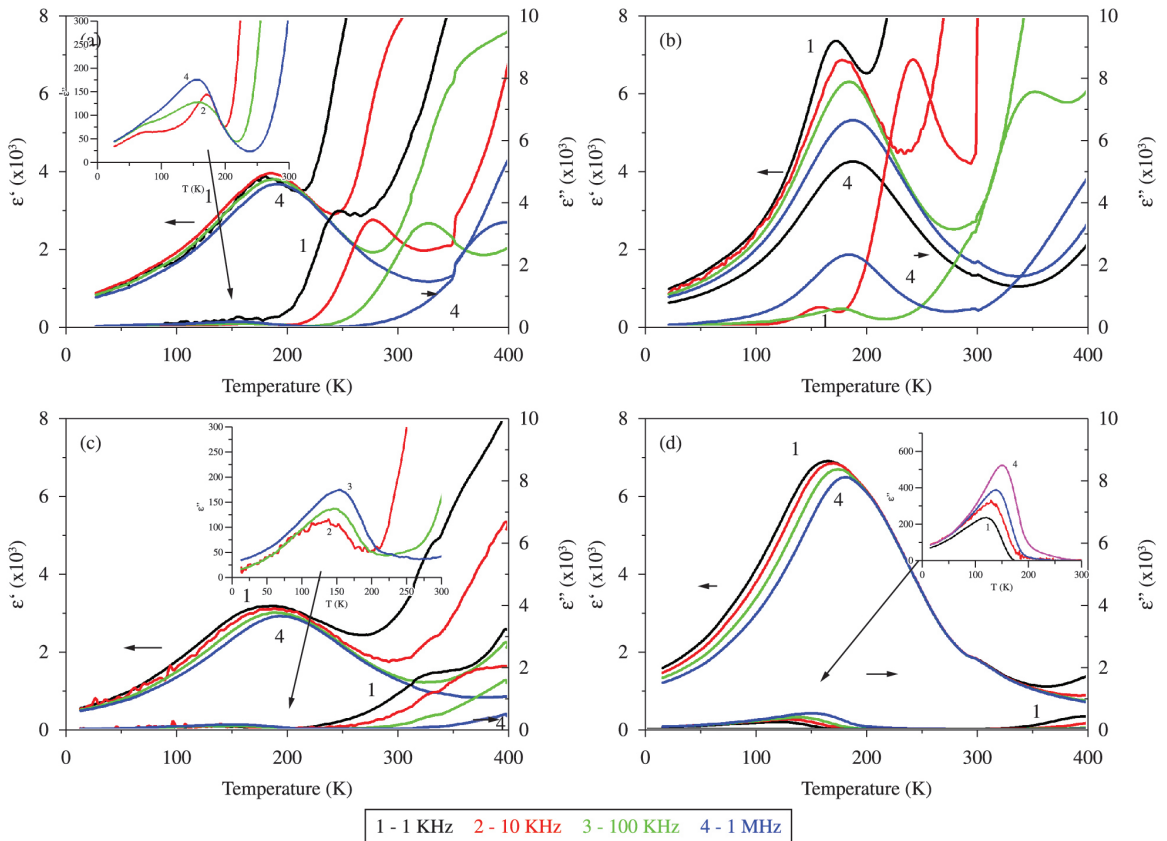


**Figure 3.** Relative Dielectric permittivity at various frequencies as a function of temperature for (a) PFW, (b) PFW-1% Gd<sub>2</sub>O<sub>3</sub>, (c) PFW-1% Cr<sub>2</sub>O<sub>3</sub> and (d) PFW-1%MnO<sub>2</sub> ceramics.

revealed that Co doping in PFW, at the level of 1-10 at %, caused a shift to lower temperatures in the transition temperature. However, not with the results reported by Szwagierczak,<sup>13</sup> where the transition temperature does not change with MnO<sub>2</sub>.

Several empirical models were proposed for describing the temperature dependence of the dielectric constant systems with relaxor behavior and diffuse phase transitions (DPT). Many authors introduced the concept of a Gaussian distribution of the Curie temperatures characteristic to the small microregions considered non-correlated<sup>14-16</sup>. However, ceramics materials generally do not present a quadratic dependence in the temperature.

To determine the characteristics of the dielectric response measurements the experimental results can be better fitted using the Santos and Eiras equation<sup>17</sup> that takes into account both the normal and the relaxor behavior of the ferroelectric phase transition

$$\epsilon' = \frac{\epsilon_m}{1 + \left(\frac{T - T_C}{\delta}\right)^\gamma} \quad (3)$$

Where  $\gamma$  and  $\delta$  are constants that describe the diffusivity of the FE transition, in special the parameter  $\gamma$  varies from 1 to 2 indicating the character of the phase transition:

from normal (1) to complete diffuse phase transition-DFT (2).  $\epsilon_m$  is the maximum of the dielectric permittivity and  $T_C$  is considered as representative of the phase transition temperature. In this way, the experimental results can be fitted as well at temperatures higher than  $T_{C\_e}$  as at some temperature interval bellow  $T_{C\_e}$ . In despite of this, here we present in Figure 4, for better visualization, the curves with adjusted parameter in all temperature interval. The dot curves in Figure 4 corresponds to the best fit of the experimental results using Equation 3. The values for  $T_{C\_e}$ ,  $\delta$  and  $\gamma$  are presented in Table 2.

The parameter  $\gamma$  shows no significant differences ( $\gamma \sim 1.94-2$ ) between non-doped and doped PFW samples. These  $\gamma$  values are characteristic of the broadened peaks observed in Figure 3, indicating that the phase transition should be classified as incomplete DPT for all studied materials. However, the  $\delta$  parameter displays a small difference between doped and pure samples, indicating that the diffusivity decreases for Gd and Mn doped samples and increases with Cr doping. Likewise, no tendency is observed on either  $\delta$  or  $\gamma$  parameters for magnetic ions doped PFW systems. The transition temperatures shift ( $\Delta T_m = T@1\text{GHz} - T@1\text{kHz}$ ) values in Cr and Gd doped samples are lower than in non-doped and Mn doped samples. Permittivity values and transition temperatures for all studied materials are reported in Table 2. As may be appreciated, the value

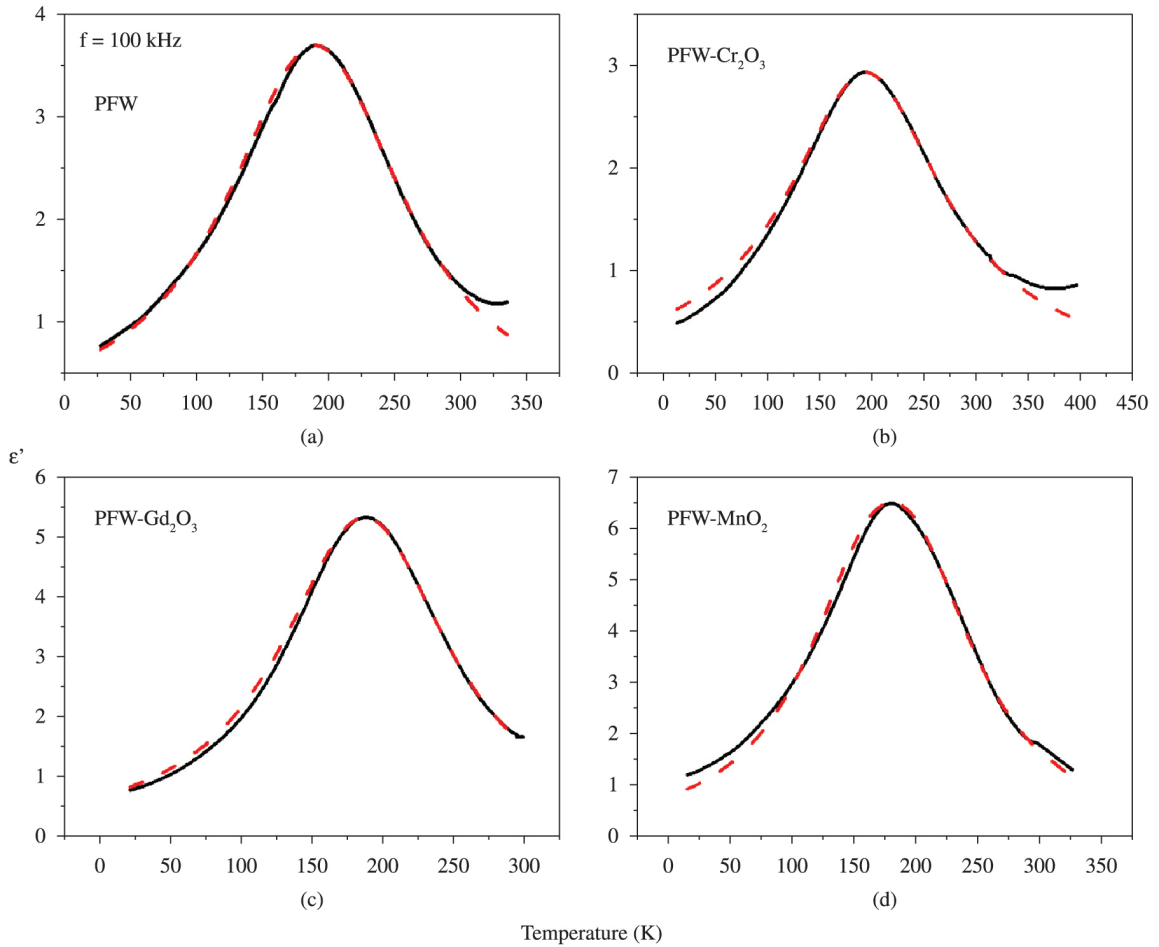


**Figure 4.** Experimental and Equation 3 generated curves with fit parameters dielectric constant as a function of temperature at 1 MHz for (a) PFW, (b) PFW-1%  $\text{Gd}_2\text{O}_3$ , (c) PFW-1%  $\text{Cr}_2\text{O}_3$  and (d) PFW-1% $\text{MnO}_2$  ceramics.

**Table 2.** Values of some dielectric properties and phase transitions parameters obtain from dielectric permittivity curve.

Sample	$E_{\max}@1\text{MHz}$	$T_c@1\text{KHz(K)}$	$E_{\max}@1\text{GHz}$	$T_c@1\text{GHz(K)}$	$\Delta T_c$	$\gamma$	$\delta$	$T_N(\text{K})$
PFW	3696	189	3264	235	46	2.00	82	325
PFW- $\text{Cr}_2\text{O}_3$	2937	194	1679	205	11	1.94	93	334
PFW- $\text{Gd}_2\text{O}_3$	5332	186	3696	204	18	2.00	72	332
PFW- $\text{MnO}_2$	6529	165	3190	203	38	2.00	73	326

of  $\epsilon_m$  for doped PFW is higher than the value for non doped ceramics, except in the Cr doped case. Increase in the dielectric constant can be attributed to the fact that Mn and Gd doping increases create B site vacancies in the PFW lattice, thereby facilitating the mobility of the ferroelectric domain walls, as in the case donor doping in PZT. In another side, Cr doping seems decrease this mobility. However, due the big dispersion observed, mainly for Gd doped samples, the dielectric contribution should be verified at higher frequencies, to suppress conductive contributions.

At higher frequencies, conductive contributions to the dielectric permittivity can be minimized, suggesting microwave dielectric spectroscopy as a more accurate tool to investigate phase transitions in multiferroic. Microwave dielectric spectroscopy has been used as a powerful

technique to probe structural phase transitions, dynamical changes in domain and nanodomain structures and lattice instabilities<sup>18-21</sup>. In this way, a systematic study of the elastic behavior also provides useful information for probing phase transitions and, therefore for detect magnetic transitions. On other hand, the presence of an elastic subsystem in the crystal leads to the emergence of electrostriction, which accompanies the FE ordering and changes the crystal size and, in turn, changes the magnetic state through magnetostriction, and vice versa.

Figure 5 illustrates the frequency dependence at MW frequencies ( $f > 10^8$  Hz) of the dielectric permittivity for PFW, at different temperatures. A well pronounced relaxation like dielectric dispersion is observed in the microwave region (around 1GHz). The microwave dielectric

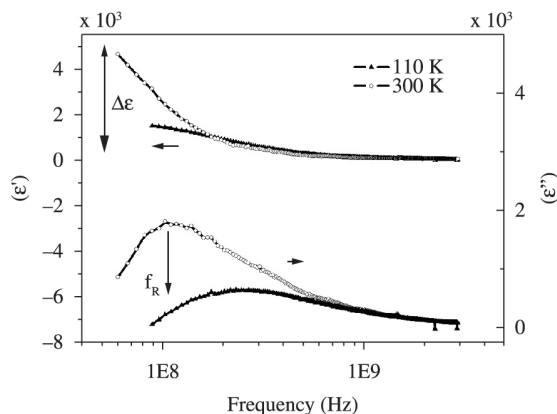


**Figure 5.** Real ( $\epsilon'$ ) and imaginary ( $\epsilon''$ ) components of the relative dielectric permittivity for PFW ceramics as a function of the frequency in the microwave range, at 110 K and 300 K.

dispersion does not vanish in the measured temperature interval and persists at temperatures up to 200 K above  $T_m$ .

The experimental data of Figure 5 can be fitted with a damped harmonic oscillator model as adopted for PLT ceramics, where  $\epsilon(f, T)$  takes the form<sup>19</sup>:

$$\epsilon(f, T) = \epsilon_{\text{inf}} + \frac{\Delta\epsilon f_R^2}{f_R^2 - f^2 + i\gamma f} \quad (4)$$

where  $\Delta\epsilon(f, T) = \epsilon(f_0, T) - \epsilon(f_{\text{INF}}, T)$  ( $f_0 \ll f_R \ll f_{\text{INF}}$ ) is the dielectric strength,  $f_R(T)$  the characteristic frequency,  $\gamma(T)$  a damping coefficient and  $\epsilon_{\text{INF}}(T)$  the high-frequencies contribution by phonons and electronic polarization.  $\epsilon(f_0, T)$  should be interpreted here as the dielectric permittivity at frequencies lower than  $f_R$ , without any additional contribution (due to phase transitions or conductive contributions).

The temperature dependence for  $\Delta\epsilon$  and  $f_R$ , reversible in the cooling and heating cycles, is shown in Figure 6(a) and (b) for all samples. The observed temperature dependence of  $f_R$  and  $\Delta\epsilon$  around 200 K,  $f_R$  reaches a minimum value, while  $\Delta\epsilon$  goes through a maximum, is associated with that of the dielectric permittivity peak, observed in RF range (Figure 3). Otherwise, remarkable are also the change of  $f_R$  curve around 330 K, which are correlated to the secondary maximums of  $\Delta\epsilon$ . These secondary maximums cannot be detected in the radio frequency dielectric measurements (Figure 3), probably because it is masked by conductive contributions superposed to the dielectric response. The same anomalies could be observed in Figure 6c, where the dielectric constant at high frequencies (1GHz) is represented. In this sense, is shown that avoiding conductive contributions at high temperatures, the dielectric anomaly observed around 330 K coincides very well with the temperature of the paramagnetic-antiferromagnetic ordering ( $T_{N1} \approx 340$  K). Therefore, based on our previous results in multiferroic systems,<sup>20,22</sup> this dielectric anomaly in the PFW system results from a magnetoelectric contribution via strain, due to a spin-lattice coupling (magnetostriction), in the paramagnetic-antiferromagnetic ordering.

Comparing the magnetic ordering temperature of the samples, results that while  $T_N$  increases for samples

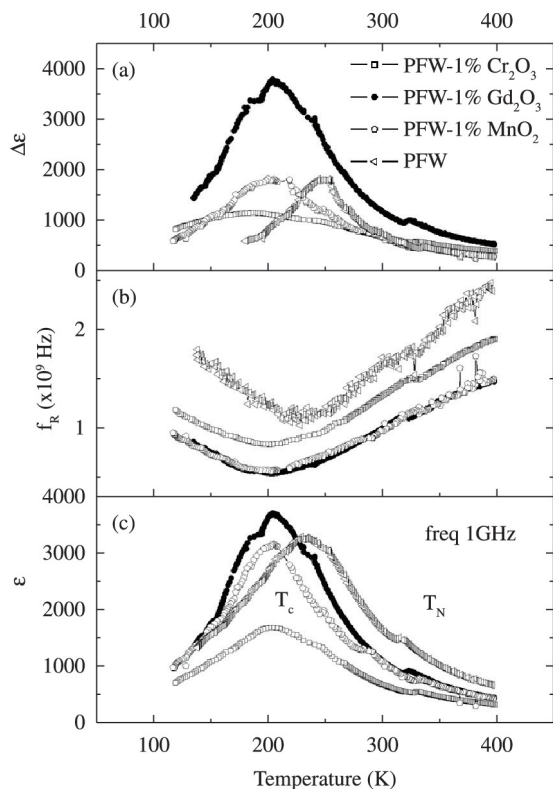


**Figure 6.** Temperature dependence of the characteristic coefficients of the microwave dispersion in PFW doping ceramics (a) dielectric strength ( $\Delta\epsilon$ ), characteristic frequency ( $f_R$ ) and (c) dielectric susceptibility at 1GHz.

doped with gadolinium and chromium (334 and 332K, respectively),  $T_N$  decreases for samples doped with manganese (326 K).

We summarize the principal results obtained from all measurement as follows:

- i) A two-stage solid-state reaction turned out to be appropriated for the formation of the majoritarian PFW phase as well for “pure” PFW as for magnetic doped ceramics, with low percentage of spurious phase and high density (>98%);
- ii) Doping decrease the lattice parameter but no systematic variation of grain size was observed;
- iii) All doping increased DC electric resistivity of PFW ceramics. It is remarkable the change induced by Mn doping, where the electrical resistivity is 8 orders of magnitude higher than in pure samples;
- iv) The magnetic ions introduced in PFW lattice induced changes of less than 10% in the ferroelectric ordering temperatures, but did not change the character of the phase transition. The value of the dielectric constant increases for Gd and Mn doping, and decrease for Cr doping;
- v) MW dielectric responses were investigated in magnetic ions doped Pb(Fe<sub>2/3</sub>W<sub>1/3</sub>)O<sub>3</sub> multiferroic ceramics. A dielectric dispersion occurs in the frequency range of 100MHz-3GHz for all samples and at different temperatures;

- vi) At low temperatures, dielectric microwave measurements show the ferroelectric phase transition, close to 205 K;
- vii) At high temperatures, dielectric microwave measurements prove the coupling between the elastic and magnetic parameters. Ion doping change less than 8% the temperature of magnetic phase transition.

Despite all ions improved dielectric and electric properties in PFW multiferroic ceramics, without change the characteristics of the ferroelectric and magnetic phase transitions temperatures, our results demonstrated that Mn doping is the best option to suppress conductive contributions, which is supported by the increase in the electric resistivity.

#### 4. Conclusions

Structural, electric and dielectric properties were investigated in “pure” and with MnO<sub>2</sub>, Gd<sub>2</sub>O<sub>3</sub> or Cr<sub>2</sub>O<sub>3</sub> doped Pb(Fe<sub>2/3</sub>W<sub>1/3</sub>)O<sub>3</sub> ceramics. Dielectric and ferroelectric properties could be “tuned” by the adding magnetic

ions to PFW. The microstructure of PFW did not change significantly on substitution of Mn/Cr ions at the Fe-sites. Detailed studies of dielectric constant and loss as a function of temperature at different frequencies showed that all compounds present a relaxor like response with T<sub>m</sub> below room temperature. The maximum dielectric constant (ε<sub>m</sub>) increases in doped PFW, except for the Cr doped samples. High frequencies measurements showed changes smaller than 8% in T<sub>C</sub> and T<sub>N</sub> with doping, and all doped samples keeping the main characteristics of the PFW ferroelectric relaxor phase transitions, improving electric properties.

#### Acknowledgments

The authors wish to thank CNPq and FAPESP for the financial support, to Prof. Yvonne P. Mascarenhas (Crystallography Group of the Physics Institute of USP-São Carlos) for the use of the XRD Lab facilities and to Mr. Francisco J. Picon and Mrs. Natalia A. Zanardi for the technical assistance.

#### References

1. Takahashi S. Internal Bias Field Effects in Lead Zirconate-Titanate Ceramics Doped with Multiple Impurities. *Japanese Journal of Applied Physics*. 1981; 20(1):95-101. <http://dx.doi.org/10.1143/JJAP.20.95>.
2. Takahashi S. Effects of Impurity Doping in Lead Zirconate-Titanate Ceramics. *Ferroelectrics*. 1982; 41(1):143-156. <http://dx.doi.org/10.1080/00150198208210617>.
3. Uchino K, Zheng J, Joshi A, Chen Y-H, Yoshikawa S, Hirose S, et al. High power characterization of piezoelectric materials. *Journal of Electroceramics*. 1998; 2(1):33-40. <http://dx.doi.org/10.1023/A:1009962925948>.
4. Eerenstein W, Mathur ND and Scott JF. Multiferroic and magnetoelectric materials. *Nature*. 2006; 442(7104):759-765. <http://dx.doi.org/10.1038/nature05023>. PMID:16915279
5. Chupis IE. Progress in studying ferroelectromagnetic crystals. *Low Temperature Physics*. 2010; 36(6):477-488. <http://dx.doi.org/10.1063/1.3462535>.
6. Spaldin NA and Fiebig M. Materials science. The renaissance of magnetoelectric multiferroics. *Science*. 2005; 309(5733):391-392. <http://dx.doi.org/10.1126/science.1113357>. PMID:16020720
7. Hill NA. Why are there so few magnetic ferroelectrics? *The Journal of Physical Chemistry B*. 2000; 104(29):6694-6709. <http://dx.doi.org/10.1021/jp000114x>.
8. Spaldin N, Cheong SW and Ramesh R. Multiferroics erratum. *Physicstoday*. 2011; 64(2):9-9. <http://dx.doi.org/10.1063/1.3582237>.
9. Fraygola B, Coelho AA, Garcia D and Eiras JA. Magnetic and ferroelectric phase coexistence in multiferroics PFW-PT ceramics. *Processing and Applications of Ceramics*. 2012; 6(1):65-75. <http://dx.doi.org/10.2298/PAC1201065F>.
10. Fraygola B, Coelho AA, Garcia D and Eiras JA. Magnetic and Dielectric Properties of Multiferroic (1-x)Pb(Fe<sub>2/3</sub>W<sub>1/3</sub>)O<sub>3</sub>-xPbTiO<sub>3</sub> Ceramics Prepared Via a Modified Two-stage Solid-state Reaction. *Materials Research-Ibero-American Journal of Materials*. 2011; 14:434-441.
11. Swartz SL and ShROUT TR. Fabrication of perovskite lead magnesium niobate. *Materials Research Bulletin*. 1982; 17(10):1245-1250. [http://dx.doi.org/10.1016/0025-5408\(82\)90159-3](http://dx.doi.org/10.1016/0025-5408(82)90159-3).
12. Miranda C, Vilarinho PM and Zhou LQ. Dielectric properties of cobalt and chromium doped lead iron tungstate relaxer ceramics. *Ferroelectrics*. 1999; 223(1):269-276. <http://dx.doi.org/10.1080/00150199908260580>.
13. Szwagierczak D and Kulawik J. Influence of MnO<sub>2</sub> and Co<sub>3</sub>O<sub>4</sub> dopants on dielectric properties of Pb(Fe<sub>2/3</sub>W<sub>1/3</sub>)O<sub>3</sub> ceramics. *Journal of the European Ceramic Society*. 2005; 25(9):1657-1662. <http://dx.doi.org/10.1016/j.jeurceramsoc.2004.05.022>.
14. Cross LE. Relaxor Ferroelectrics. *Ferroelectrics*. 1987; 76(1):241-267. <http://dx.doi.org/10.1080/00150198708016945>.
15. Uchino K. Relaxor Ferroelectrics. *Journal of the Ceramic Society of Japan*. 1991; 99(1154):829-835. <http://dx.doi.org/10.2109/jcersj.99.829>.
16. Isupov VA. Diffuse Ferroelectric Phase-Transitions and PLZT Ceramics. *Ferroelectrics*. 1992; 131(1):41-48. <http://dx.doi.org/10.1080/00150199208223390>.
17. Santos IA and Eiras JA. Phenomenological description of the diffuse phase transition in ferroelectrics. *Journal of Physics Condensed Matter*. 2001; 13(50):11733-11740. <http://dx.doi.org/10.1088/0953-8984/13/50/333>.
18. Maglione M, Böhmer R, Loidl A and Höchli UT. Polar relaxation mode in pure and iron-doped barium titanate. *Physical Review B: Condensed Matter and Materials Physics*. 1989; 40(16):11441-11444. <http://dx.doi.org/10.1103/PhysRevB.40.11441>. PMID:9991740
19. Guerra JDS, Lente MH, and Eiras JA. Microwave dielectric dispersion process in perovskite ferroelectric systems. *Applied Physics Letters*. 2006; 88(10):102905-1-102905-3.
20. Lente MH, Guerra JDS, Souza GKS, Fraygola BM, Raigoza CFV, Garcia D, and Eiras JA. Nature of the magnetoelectric coupling in multiferroic Pb(Fe(1/2)Nb(1/2))O<sub>3</sub> ceramics. *Physical Review B*. 2008; 78(5):054109-1-054109-6.
21. Grigas J. Microwave Dielectric Spectroscopy of Ferroelectrics. *Ferroelectrics*. 2009; 380(1):113-121. <http://dx.doi.org/10.1080/00150190902876249>.
22. Fraygola B, Coelho AA, Garcia D and Eiras JA. Magnetic ordering and instability investigation of multiferroic Pb(Fe<sub>2/3</sub>W<sub>1/3</sub>)O<sub>3</sub> ceramics by microwave dielectric spectroscopy. *Solid State Communications*. 2011; 151(23):1810-1813. <http://dx.doi.org/10.1016/j.ssc.2011.08.020>.